



Adsorption proprieties and inhibition of mild steel corrosion in HCl solution by the essential oil from fruit of Moroccan *Ammodaucus leucotrichus*

M. Manssouri¹, Y. El Ouadi², M. Znini¹, J. Costa³, A. Bouyanzer²
J-M. Desjobert³, L. Majidi^{1*}

¹ Université My Ismail, Laboratoire des Substances Naturelles & Synthèse et Dynamique Moléculaire, Faculté des Sciences et Techniques, BP 509, 52003, Errachidia, Morocco.

² Université Mohamed Premier, Laboratoire de Chimie Appliquée et Environnement, Faculté des Sciences, Oujda, Morocco.

³ Université de Corse, CNRS-UMR 6134, Laboratoire de Chimie des Produits Naturels, BP 52, 20250 Corti, France.

Received 2 Feb 2015, Revised 22 Feb 2015, Accepted 23 Feb 2015

* Corresponding author. E-mail: lmajidi@yahoo.fr

Abstract

The essential oil from the fruits of *Ammodaucus leucotrichus* (AL oil) was studied by Gas Chromatography (GC) and Gas Chromatography-Mass Spectrometry (GC/MS). 10 components were identified accounting 94.7% of the total oil, which peryllaldehyde (73.5%) and limonene (12.5%) were the major compounds. The inhibitive effect of this essential oil on the corrosion of mild steel in 1M HCl solution was investigated by weight loss measurement as well as potentiodynamic polarization and electrochemical impedance spectroscopy (EIS) techniques. From loss measurements, it is clear that inhibition efficiency values increased with increase in inhibitor concentration but decreased with increase in temperature. Polarization measurements showed that the studied inhibitor is mixed type with significant reduction of cathodic and anodic current densities. The results of EIS measurements indicated that the corrosion of steel is mainly controlled by the charge transfer process. Various activation and adsorption thermodynamic parameters are evaluated and discussed. Linearity of Langmuir isotherm adsorptions indicated the monolayer formation of inhibitor on mild steel surface.

Keywords: *Ammodaucus leucotrichus*, Essential oil, peryllaldehyde, limonene, Mild steel, Corrosion inhibition.

1. Introduction

Corrosion is gradual destruction of a material because of its reaction with environment. This major industrial problem has attracted many investigators in recent years [1]. Indeed, corrosion control is an essential issue from application point of view and it has been reported that inhibitors are needed to be used which act as a barrier to reduce the aggressiveness of the environments against the corrosion attack [2]. An attempt to find corrosion inhibitors that are environmentally safe and readily available has been a growing trend in the use of natural products such as essential oils as corrosion inhibitors for metals in acid cleaning processes. The essential oils are rich sources of molecules that have appreciably high inhibition efficiency and hence termed as “Green Inhibitors”. These organic compounds can adsorb on the metal surface, block the active sites on the surface and thereby reduce the corrosion rate [3].

In our laboratory, much work has been conducted to study the inhibition by some plant leaves extract on the corrosion of steel in acidic media [4-10]. In continuation of our previous studies, the present work devotes to investigate the corrosion inhibition of *Ammodaucus leucotrichus* fruit essential oil.

Ammodaucus leucotrichus is a species of flowering plant in the *Apiaceae* family and the sole member of the genus *Ammodaucus*. It is a small annual plant, 10-12 cm. high, glabrous with erect, finely striated stems. The leaves are finely dissected and slightly fleshy. The flowers are grouped in umbels of 2 to 4 branches. The flowers are small, with 5 free petals. The fruit is a di-achene, 8-10 mm. long, and is covered with dense silky white hairs. The plant has a strong smell of anise [11]. *A. leucotrichus* inhabits the maritime sands in the Saharan and sub-Saharan countries of North Africa, Morocco, Algeria and Tunisia, extending to Egypt and tropical Africa [12]. In Morocco, which locally known as “kammûn es-sofi or akâman”, the fruits are used either by the local population as a powder or in a decoction to treat gastric-intestinal pain, gastralgias and indigestion. It is also frequently used, as an infusion, for diverse infantile diseases of the digestive apparatus: dysentery, nausea, regurgitation, vomiting. It also has tonic properties for babies and is taken as an infusion or in the bath [13].

In the present study, the inhibitive effects of the essential oil from the fruits of *Ammodaucus leucotrichus* (AL oil) on corrosion of mild steels in hydrochloric acid solution were investigated for the first time. For this purpose, the oil chemical composition has been studied using GC and GC-MS. The investigation of corrosion parameters was performed by weight loss, electrochemical polarization measurements and electrochemical impedance spectroscopy. The effect of temperature was also studied and discussed.

2. Materials and methods

2.1. Plant material

The fruits of *Ammodaucus leucotrichus* were harvested around Errachidia (Morocco) and were identified by biology department of Faculty of Sciences and Technology of Errachidia (Morocco).

2.2. Essential oil isolation

The dried vegetal material (100 g) were water-distilled (3h) using a Clevenger-type apparatus according to the method recommended by the European Pharmacopoeia [14]. The yield of fruits essential oil was 1.33%.

2.3. GC analysis

GC analysis were carried out using a Perkin-Elmer Autosystem XL GC apparatus equipped with dual flame ionization detection (FID) system and fused-silica capillary columns (60 m×0.22 mmI.D., film thickness 0.25 µm), Rtx-1 (polydimethylsiloxane) and Rtx-wax (polyethyleneglycol). The oven temperature was programmed from 60°C to 230°C at 2°C/min and then held isothermally at 230°C for 35 min. Injector and detector temperature was maintained at 280°C. Samples were injected in the split mode (1/50), using helium as carrier gas (1 ml/min); the injection volume was 0.2 µL of pure oil. Component relative concentrations were calculated based on GC peak areas without using correction factors.

2.4. GC-MS analysis

Samples were also analysed using a Perkin-Elmer Turbo mass detector (quadrupole), coupled to a Perkin-Elmer Autosystem XL, equipped with fused-silica capillary columns Rtx-1 and Rtx-Wax. Carrier gas: helium (1 mL/min), ion source temperature: 150°C, oven temperature programmed from 60°C to 230°C at 2°C/min and then held isothermally at 230°C (35 min), injector temperature: 280°C, energy ionization: 70 eV, electron ionization mass spectra were acquired over the mass range 35-350 Da, split: 1/80, injection volume: 0.2 µL of pure oil.

2.5. Identification of components

The methodology carried out for identification of individual components was based on: i) comparison of calculated retention indices (RI), on polar and apolar columns, with those of authentic compounds or literature data [15]; ii) computer matching with commercial mass spectral libraries [16] and comparison of mass spectra with those of our own library of authentic compounds or literature data [15,17].

2.6. Preparation of materials

Mild steel coupons containing 0.09 wt.% (P), 0.38 wt.% (Si), 0.01 wt.% (Al), 0.05 wt.% (Mn), 0.21 wt.% (C), 0.05 wt.% (S) and the remainder iron (Fe) used for weight loss measurements. The surface preparation of the mild steel coupons (2 cm x 2 cm x 0.05 cm) was carried out with emery papers by increasing grades (400, 600 and 1200 grit size), then degreased with AR grade ethanol and dried at room temperature before use. The aggressive solutions of 1 M HCl was prepared by dilution of analytical grade 37% HCl with double distilled water. The concentration range of the AL oil was 0.25-3 g/L. This concentration range was chosen upon the maximum solubility of AL oil. All reagents used for the study were of analytical grade.

2.7. Weight loss measurements

Weight loss tests were carried out in a double walled glass cell equipped with a thermostat-cooling condenser. The solution volume was 100 mL with and without the presence of different concentrations of AL oil ranging from 0.25 to 3 g/L at various temperatures (308-343 K). After 6 h of immersion, the specimens of steel were carefully washed in double-distilled water, dried and then weighed. The rinse removed loose segments of the film of the corroded samples. Triplicate experiments were performed in each case and the mean value of the weight loss is reported using an analytical balance (precision ± 0.1 mg). Weight loss allowed us to calculate the mean corrosion rate as expressed in $\text{mg}\cdot\text{cm}^{-2}\cdot\text{h}^{-1}$.

The corrosion rate (W_{corr}) and inhibition efficiency E_w (%) were calculated according to the Eqs. (1) and (2) respectively:

$$W = \frac{\Delta m}{St} \quad (1)$$

$$E_w \% = \frac{W_{\text{corr}} - W_{\text{corr(inh)}}}{W_{\text{corr}}} \times 100 \quad (2)$$

where Δm (mg) is the specimen weight before and after immersion in the tested solution, W_{corr} and $W_{\text{corr(inh)}}$ are the values of corrosion weight losses ($\text{mg}/\text{cm}^2\cdot\text{h}$) of mild steel in uninhibited and inhibited solutions, respectively, S is the area of the mild steel specimen (cm^2) and t is the exposure time (h).

The degree of surface coverage was calculated using:

$$\theta = \frac{W_{\text{corr}} - W_{\text{corr(inh)}}}{W_{\text{corr}}} \quad (3)$$

where θ is surface coverage; $W_{\text{corr(inh)}}$ is corrosion rate for steel in presence of inhibitor, W_{corr} is corrosion rate for steel in the absence of inhibitor.

2.8. Electrochemical studies

Electrochemical measurements were carried out in a conventional three-electrode electrolysis cylindrical Pyrex glass cell. The working electrode (WE) in the form of disc cut from steel has a geometric area of 1 cm^2 and is embedded in polytetrafluoroethylene (PTFE). A saturated calomel electrode (SCE) and a disc platinum electrode were used respectively as reference and auxiliary electrodes, respectively. The temperature was thermostatically controlled at 308 K. The WE was abraded with silicon carbide paper (grade P1200), degreased with AR grade ethanol and acetone, and rinsed with double-distilled water before use.

2.9. Potentiodynamic polarization curves

Polarization curves studies were carried out using EG&G Instruments potentiostat-galvanosta (Model 263A) at 308 K without and with addition of various concentrations of AL oil (0.25-3 g/L) in 1 M HCl solution at a scan rate of 0.5 mV/sec. Before recording the cathodic polarization curves, the mild steel electrode is polarised at -800 mV for 10 min. For anodic curves, the potential of the electrode is swept from its corrosion potential after 30 min at free corrosion potential, to more positive values. The test solution was deaerated with pure nitrogen. Gas bubbling was maintained through the experiments.

In the case of polarization method the relation determines the inhibition efficiency (E_I %):

$$E_I \% = \frac{I_{\text{corr}} - I_{\text{corr(inh)}}}{I_{\text{corr}}} \times 100 \quad (4)$$

where I_{corr} and $I_{\text{corr (inh)}}$ are the corrosion current density values without and with the inhibitor, respectively, obtained by extrapolation of cathodic and anodic Tafel lines to the corrosion potential.

2.10. Electrochemical impedance spectroscopy (EIS)

The electrochemical impedance spectroscopy (EIS) measurements were carried out with the electrochemical system which included a digital potentiostat model Volta lab PGZ 100 computer at E_{corr} after immersion in solution without bubbling, the circular surface of mild steel exposing of 1 cm^2 to the solution were used as working electrode. After the determination of steady-state current at a given potential, sine wave voltage (10 mV) peak to peak, at frequencies between 100 kHz and 10 mHz were superimposed on the rest potential. Computer programs automatically controlled the measurements performed at rest potentials after 30 min of exposure.

The impedance diagrams was given in the Nyquist representation. Values of R_t and C_{dl} were obtained from Nyquist plots. The charge-transfer resistance (R_t) values are calculated from the difference in impedance at lower and higher frequencies, as suggested by Tsuru et al [18]. The inhibition efficiency got from the charge-transfer resistance was calculated by the following relation:

$$E_{R_t} \% = \frac{R'_t - R_t}{R'_t} \times 100 \quad (5)$$

where R_t and R'_t are the charge-transfer resistance values without and with inhibitor respectively. R_t is the diameter of the loop.

The double layer capacitance (C_{dl}) and the frequency at which the imaginary component of the impedance is maximum (Z_{max}) are found determined by Eq. (6):

$$C_{\text{dl}} = \frac{1}{\omega \cdot R_t} \quad \text{where } \omega = 2 \pi \cdot f_{\text{max}} \quad (6)$$

Impedance diagrams were obtained for frequency range 100 KHz –10 mHz at the open circuit potential for mild steel in 1 M HCl in the presence and absence of AL oil.

3. Results and discussion

3.1. Essential oil composition

Analysis of the essential oil from the fruits of *Ammodaucus leucotrichus* (AL oil) was carried out by GC and GC–MS using the methodologies described in the section 2. Ten components amounting to 94.7% of the total oil composition were identified by comparison of their electron ionization-mass spectra (EI-MS) and their retention indices (RI) with those of our own authentic compound library (Table 1). These compounds including five monoterpene hydrocarbons (**1-5**) and five oxygenated monoterpenes (**6-10**), whereas, we noted that the sesquiterpene compounds (hydrocarbons and oxygenated) were absent. The chemical composition of the AL oil was strongly dominated by oxygenated monoterpenes (79.7% of the total oil) with peryllaldehyde **7** (73.5%) followed by limonene **5** (12.5%) were the major components. These results were in accordance with those previously reported in literature for the volatiles from the fruits of *A. leucotrichus* subsp. *leucotrichus*, collected from in Dakhla (Morocco) [19]. The authors have identified, by GC/MS, thirteen compounds among them peryllaldehyde (63.6%) and limonene (26.8%) were the major components. The higher percentage of perillaldehyde in our samples is due to the loss of limonene during the drying stage. Probably, the plant oxidation process was initiated in the 1-methyl group of limonene, converting it to perilla alcohol and thence to the other derivatives such as perillaldehyde [20].

3.2. Weight loss measurement

The non-electrochemical technique of weight loss was done in order to determine the corrosion rate (W) and percentage of inhibition (E_w) at various concentrations of AL oil and at different temperatures (Table 2).

The results indicated that the corrosion rate (W) of mild steel decreased continuously with increasing the inhibitor concentration, ie, the corrosion of steel was retarded by AL oil, or the inhibition enhances with the inhibitor concentration. This behaviour was due to the fact that the adsorption coverage of inhibitor on steel

surface increases with the inhibitor concentration. Also, the corrosion rate (W) increases with temperature both in uninhibited and inhibited solutions, especially goes up more rapidly in the absence of inhibitor. These results confirm that AL oil acts as an effective inhibitor in the range of temperature studied (Fig. 1).

Table 1: Chemical composition of *A. leucotrichus* fruit essential oil from Morocco.

N ^a	Components	RI l ^b	RI a ^c	RI p ^d	% ^e
1	α -Pinene	936	928	1021	1,1
2	β -Pinene	978	966	1109	0,5
3	Myrcene	987	976	1158	0,2
4	3-Carene	1010	1001	1147	0,7
5	Limonene	1025	1019	1204	12,5
6	Cuminaldehyde		1210	1781	1,6
7	Peryllaldehyde	1260	1251	1772	73,5
8	α -Terpinen-7-al		1267	1772	1,3
9	γ -Terpinen-7-al		1279	1854	1,5
10	methyl Perillate	1381	1372	1985	1,8
Total identified (Monoterpenes)					94.7
Monoterpene Hydrocarbons					15
Oxygenated Monoterpenes					79.7

^aOrder of elution are given on apolar column (Rtx-1);

^bRI l = retention indices on the apolar column (Rtx-1) in literature;

^cRI a = retention indices on the apolar column (Rtx-1) ;

^dRI p = retention indices on the polar column (Rtx-Wax);

^eRelative percentages of components (%) are calculated on GC peak areas on the apolar column (Rtx-1).

Table 2: Corrosion Parameters for mild Steel in 1 M HCl in absence and presence of different concentrations of *A. leucotrichus* fruit essential oil obtained from Weight Loss Measurements at different temperatures.

C (g/L)	308 K		313 K		323 K		333 K		343 K	
	W (mg/cm ² .h)	E _w (%)								
0	0.942	1.751	2.836	3.641	6.301
0.25	0.354	62.42	0.820	53.16	1.414	50.14	1.875	48.50	4.117	34.66
0.5	0.316	66.45	0.722	58.76	1.280	54.86	1.860	48.91	4.097	34.97
1	0.298	68.36	0.655	62.59	1.246	56.06	1.847	49.27	3.994	36.61
2	0.186	80.25	0.400	77.15	0.977	65.55	1.815	50.15	3.255	48.34
3	0.169	82.05	0.385	78.01	0.681	75.98	1.741	52.18	3.195	49.29

Moreover, the results reveal also that inhibition efficiency E_w increases sharply with increase in concentration of inhibitor, indicating that the extent of inhibition is dependent on the amount of AL oil (concentration-dependent). Also, we note that the efficiency (E_w) depends on the temperature and decreases with the rise of temperature from 308 to 343 K, and when the concentration reached to 3 g/L, E_w of AL oil reached a high value of 82.05% in 1 M HCl solution at 308 K, which represents excellent inhibitive ability of AL oil (Fig. 2). The

decrease in inhibition efficiency with increase in temperature may be attributed to the increased desorption of inhibitor molecules from metal surface and the increase in the solubility of the protective film of the reaction products precipitated on the surface of the metal that might otherwise inhibit the reaction.

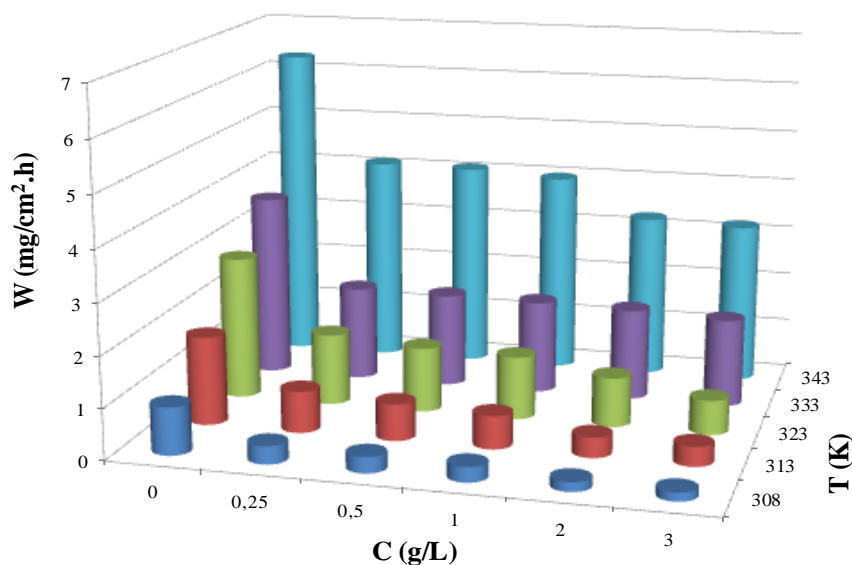


Figure 1: Variation of corrosion rate (W) as a function of temperature and concentration of *A. leucotrichus* fruit essential oil (C).

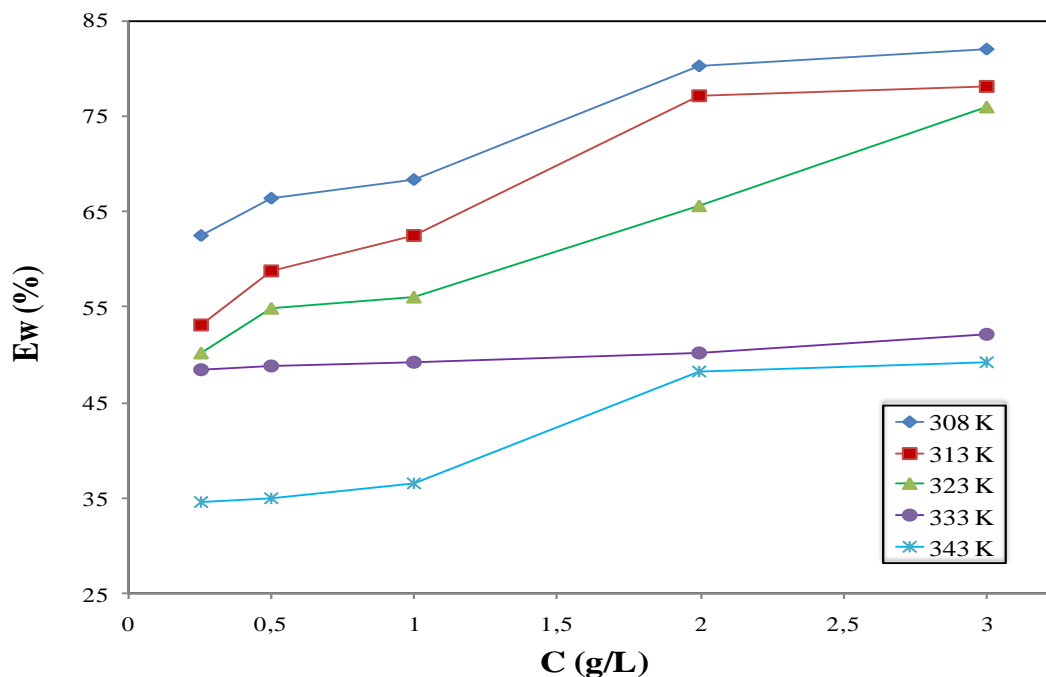


Figure 2: Relationship between inhibition efficiency (E_w) and temperature and concentration of *A. leucotrichus* fruit essential oil in 1 M HCl.

3.3. Potentiodynamic polarization curves

Potentiodynamic anodic and cathodic polarization plots for mild steel specimens in 1 M HCl solution in the absence and presence of different concentrations of AL oil at 308 K are shown in Figure 3. The respective kinetic parameters including corrosion current density (I_{corr}), corrosion potential (E_{corr}), cathodic and anodic Tafel slopes (β_c , β_a) and inhibition efficiency (IE%) are given in Table 3.

It is clear from Figure 3 that the addition of AL oil has an inhibitive effect in the both anodic and cathodic parts of the polarization curves. This indicates a modification of the mechanism of cathodic hydrogen evolution as well as anodic dissolution of steel, which suggest that inhibitor powerfully inhibits the corrosion process of mild steel, and its ability as corrosion inhibitor is enhanced as its concentration is increased. In addition, the parallel cathodic Tafel curves in Figure 3 show that the hydrogen evolution is activation-controlled and the reduction mechanism is not affected by the presence of this inhibitor.

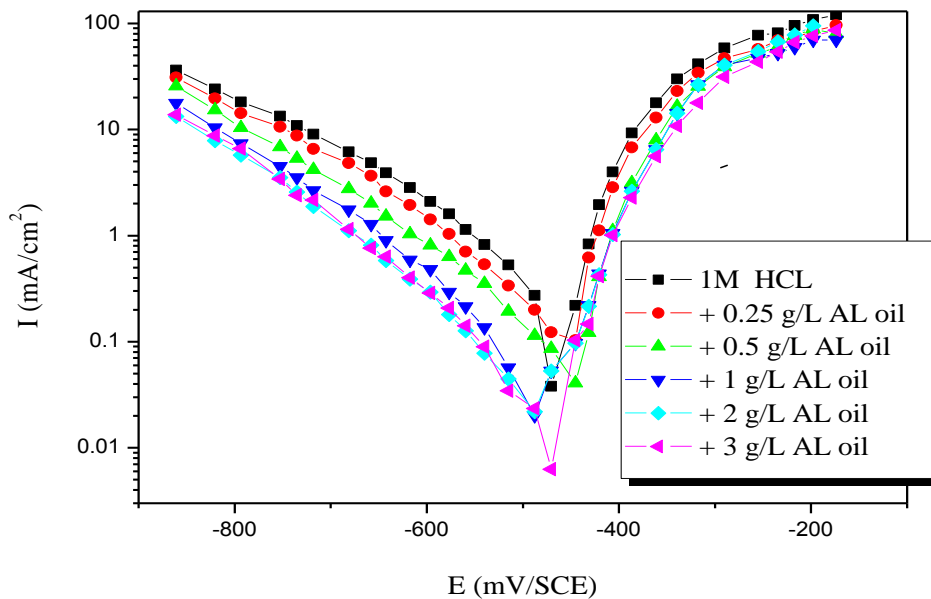


Figure 3: Anodic and cathodic polarization curves of mild steel in solutions of 1 M HCl in the presence and absence of different concentrations of *A. leucotrichus* fruits essential oil.

Table 3: Polarization parameters for the mild steel in 1 M HCl containing different concentrations of *A. leucotrichus* fruit essential oil.

C (g/L)	$-E_{\text{corr}}$ (mV/SCE)	I_{corr} (mA/cm ²)	$-\beta_c$ (mV)	β_a (mV)	IE%
0	477.7	0.3335	158.1	76.8	--
0.25	472.8	0.1520	158.0	55.0	54.42
0.50	456.0	0.1407	144.4	44.7	57.81
1	442.8	0.1098	179.0	39.0	67.07
2	500.3	0.0588	132.3	66.7	82.36
3	454.1	0.0498	133.0	49.5	85.06

From Table 3, it is clear that increasing concentration of the inhibitor resulted in a decrease in corrosion current densities (I_{corr}) and an increase in inhibition efficiency (IE %), reaching its maximum value, 85.06%, at 3 g/L. This behavior suggests that the inhibitor adsorption protective film formed on the carbon steel surface tends to be more and more complete and stable. The presence of AL oil caused a slight shift of corrosion potential towards the positive values compared to that in the absence of inhibitor. In literature, it has been also reported that if the displacement in E_{corr} is > 85 mV the inhibitor can be seen as a cathodic or anodic type inhibitor and if the displacement of E_{corr} is < 85 mV, the inhibitor can be seen as mixed type [21]. In our study, the maximum

displacement in E_{corr} value was 34.9 mV for MR oil which indicates that the inhibitor acts as mixed type inhibitor with predominantly control of anodic reaction.

3.4. Electrochemical impedance spectroscopy (EIS)

The corrosion of mild steel in 1 M HCl solution in the presence of AL oil was investigated by EIS at room temperature after an exposure period of 30 min. Nyquist plots for mild steel obtained at the interface in the absence and presence of AL oil at different concentrations is given in Figure 4.

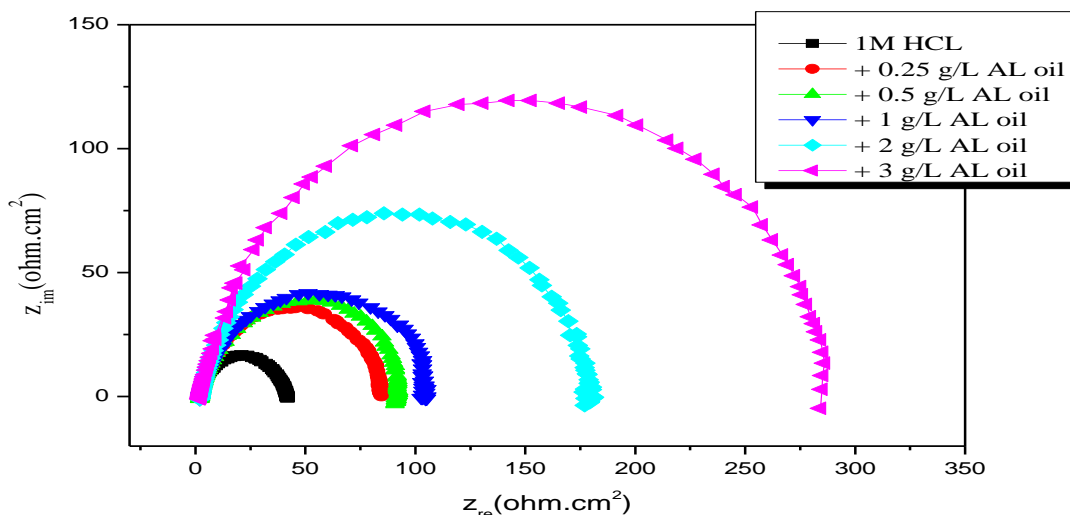


Figure 4: Nyquist plots for mild steel in 1 M HCl in the presence and absence of different concentrations of *A. leucotrichus* fruit essential oil.

As shown in Figure 4, in uninhibited and inhibited 1 M HCl solutions, the impedance spectra exhibit one single capacitive loop, which indicates that the corrosion of steel is mainly controlled by the charge transfer process [22]. It is noted that these capacitive loops in 1 M HCl solutions are not perfect semicircles which can be attributed to the frequency dispersion effect as a result of the roughness and inhomogeneous of electrode surface [23]. Furthermore, the diameter of the capacitive loop in the presence of inhibitor is larger than that in blank solution, and enlarges with the inhibitor concentration. This means that the impedance of inhibited substrate increases with the inhibitor concentration, and leads to good inhibitive performance.

The EIS results of these capacitive loops are simulated by the equivalent circuit shown in Figure 5 to pure electric models that could verify or rule out mechanistic models and enable the calculation of numerical values corresponding to the physical and/or chemical properties of the electrochemical system under investigation. In the electrical equivalent circuit, R_s is the electrolyte resistance, R_t the charge transfer resistance and C_{dl} is the double layer capacitance.

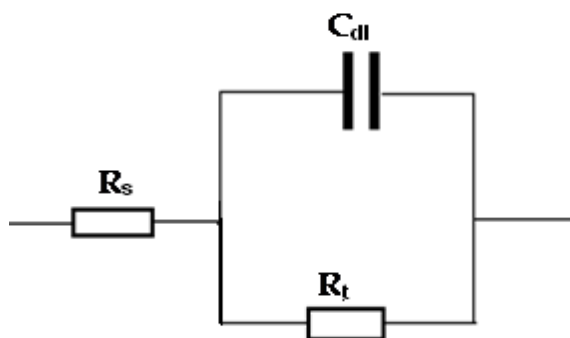


Figure 5: Equivalent circuit used to fit the EIS data of mild steel in 1 M HCl without and with different concentrations of *A. leucotrichus* fruits essential oil.

The electrochemical parameters of R_t , C_{dl} and f_{max} derived from Nyquist plots and inhibition efficiency E_{Rt} (%) are calculated and listed in Table 4.

Table 4: Electrochemical parameters for mild steel in 1 M HCl in presence and absence of different concentrations of *A. leucotrichus* fruit essential oil.

C (g/L)	- E_{corr} (mV/SCE)	R_t ($\Omega \cdot cm^2$)	f_{max} (Hz)	C_{dl} ($\mu F \cdot cm^2$)	E_{Rt} %
0	477.7	40.42	63.30	62.20	--
0.25	472.8	81.87	31.65	61.42	50.63
0.50	456.0	85.13	40.00	46.73	52.52
1	442.8	100.6	40.00	39.55	59.82
2	500.3	176.7	28.10	32.05	77.12
3	454.1	282.0	17.86	31.59	85.66

From the impedance data (Table 4), it was clear that:

- (i) R_t values in the presence of the AL oil were always greater than their values in the absence of the inhibitor molecules. This means that, this inhibitor was acting as adsorption inhibitor;
- (ii) charge transfer resistance, R_t , values were increased in the presence of the inhibitor and consequently the inhibition efficiency (E_{Rt} %) increases to 85.66% at 3 g/L, which indicates a reduction in the steel corrosion rate;
- (iii) values of double layer capacitance, C_{dl} , are also brought down to the maximum extent in the presence of inhibitor (31.59 $\mu F \cdot cm^2$ at 3 g/L) and the decrease in the values of C_{dl} follows the order similar to that obtained for I_{corr} in this study.

3.5. Kinetic/Activation parameters

In order to calculate activation parameters of the corrosion reaction such as activation energy $E^{\circ a}$, activated entropy $\Delta S^{\circ a}$ and activation enthalpy $\Delta H^{\circ a}$ for the corrosion of mild steel in acid solution in absence and presence of different concentrations of AL oil, the Arrhenius equation (7) and its alternative formulation called transition state equation (8) were employed [24].

$$W = A \exp\left(-\frac{E_a^{\circ}}{RT}\right) \quad (7)$$

$$W = \frac{RT}{Nh} \exp\left(\frac{\Delta S_a^{\circ}}{R}\right) \exp\left(-\frac{\Delta H_a^{\circ}}{RT}\right) \quad (8)$$

where $E^{\circ a}$ is the apparent activation corrosion energy, T is the absolute temperature, R is the universal gas constant, A is the Arrhenius pre-exponential factor, h is the Planck's constant, N is the Avogadro's number, $\Delta S^{\circ a}$ is the entropy of activation and $\Delta H^{\circ a}$ is the enthalpy of activation.

Plotting the logarithm of the corrosion rate (W) versus reciprocal of absolute temperature, the activation energy can be calculated from the slope ($-E^{\circ a}/R$). Figure 6 shows the variations of $\ln(W)$ with the presence and absence of inhibitor with the ($1/T$).

The logarithm of the corrosion rate of steel $\ln(W)$ can be represented as straight-lines function of ($10^3/T$) with the linear regression coefficient (R^2) was close to 1, indicating that the corrosion of steel in hydrochloric acid without and with inhibitor follows the Arrhenius equation. The activation energy ($E^{\circ a}$) values were calculated from the Arrhenius plots (Figure 6) and the results are shown in Table 5.

Further, using Eq. (8), plots of $\ln(W/T)$ versus $10^3/T$ gave straight lines (Figure 7) with a slope of ($-\Delta H^{\circ a}/R$) and an intercept of ($\ln(R/Nh) + (\Delta S^{\circ a}/R)$) from which the values of $\Delta H^{\circ a}$ and $\Delta S^{\circ a}$ were calculated and are listed in Table 5.

The activation energies in the presence of AL oil were observed higher than those in uninhibited acid solution (Table 5). This explains that the energy barrier of corrosion reaction increases with the concentration of AL oil. It is clear from equation (7) that corrosion rate is influenced by E_a° . Generally, higher E_a° value leads to the lower corrosion rate. In addition, the value of activation energy that is around 40–80 $\text{KJ}\cdot\text{mol}^{-1}$ can be suggested to obey the physical adsorption (physisorption) mechanism [25]. Physisorption is often related with this phenomenon, where an adsorptive film of electrostatic character is formed on the mild steel surface.

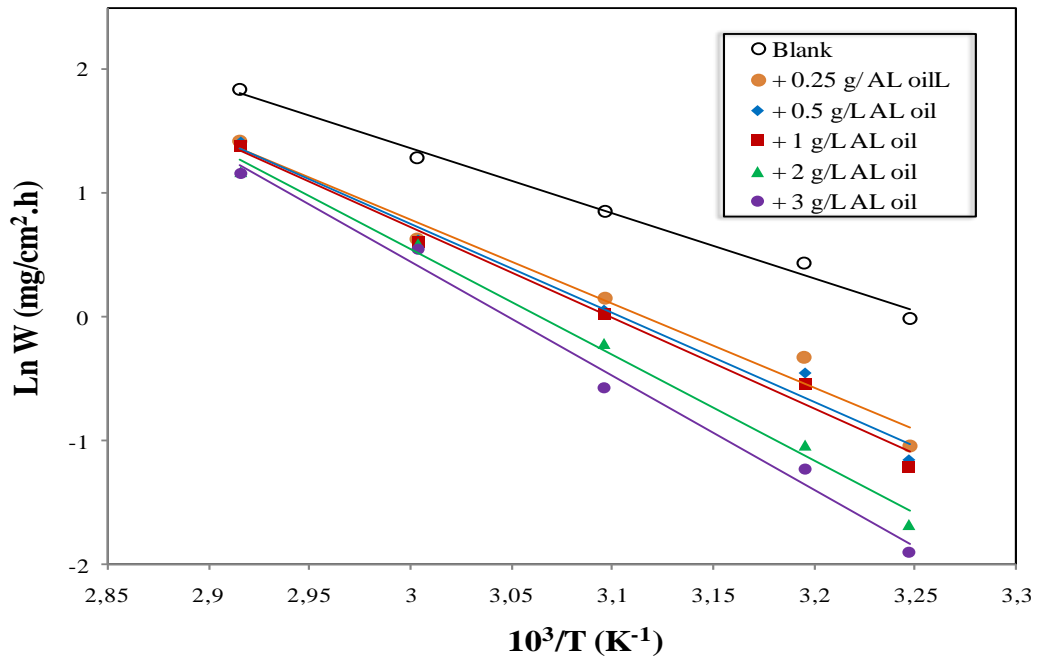


Figure 6: Arrhenius plots for mild steel corrosion rates (W_{corr}) in 1 M HCl in the absence and presence of different concentrations of *A. leucotrichus* fruit essential oil.

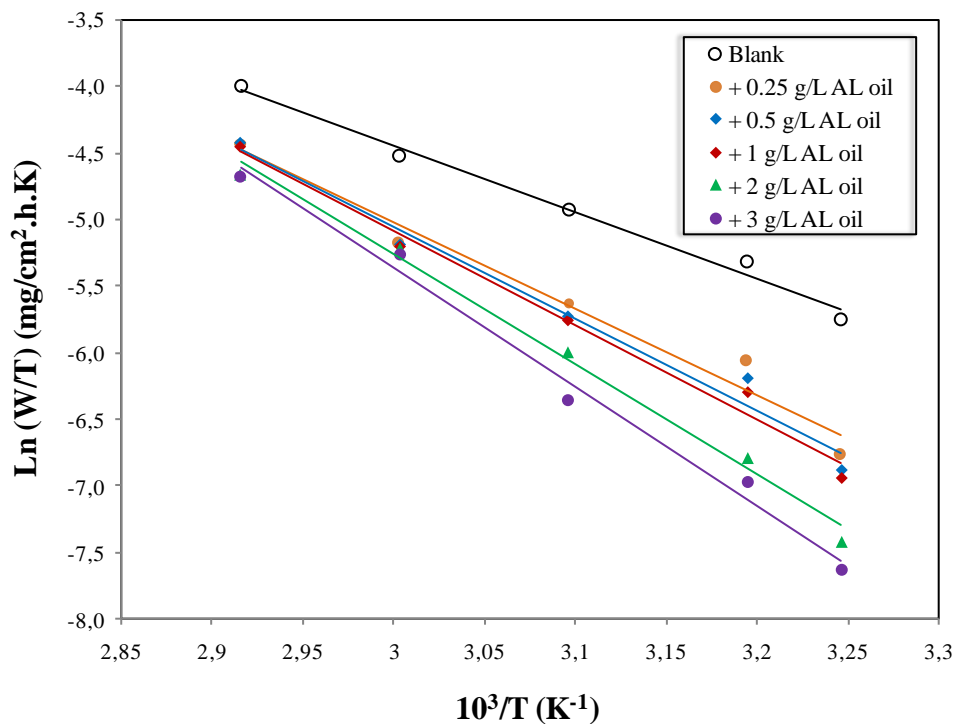


Figure 7: Transition-state plot for mild steel corrosion rates (W_{corr}) in 1 M HCl in absence and presence of different concentrations of *A. leucotrichus* fruit essential oil.

Table 5: Activation parameters $E^{\circ}a$, $\Delta S^{\circ}a$, $\Delta H^{\circ}a$ of the dissolution of mild steel in 1 M HCl in the absence and presence of different concentrations of *A. leucotrichus* fruit essential oil.

C (g/L)	$E^{\circ}a$ (KJ. mol ⁻¹)	$\Delta H^{\circ}a$ (KJ.mol ⁻¹)	$E^{\circ}a-\Delta H^{\circ}a$ (KJ. mol ⁻¹)	$\Delta S^{\circ}a$ (J. mol ⁻¹ .K ⁻¹)
0	44.05	41.34	2.71	-110.66
0.25	56.28	53.58	2.7	-78.79
0.50	59.67	56.98	2.69	-68.89
1	61.25	58.55	2.7	-64.40
2	71.21	68.51	2.7	-35.94
3	76.54	73.85	2.69	-20.8

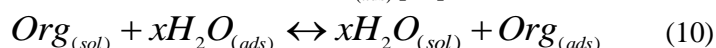
The positive value of enthalpy of activation ($\Delta H^{\circ}a$) in the absence and presence of various concentration of inhibitor reflects the endothermic nature of mild steel dissolution process meaning that dissolution of steel is difficult. It is evident from the table that the value of $\Delta H^{\circ}a$ increased in the presence of the inhibitor than the uninhibited solution indicating higher protection efficiency. This may be attributed to the presence of energy barrier for the reaction, hence the process of adsorption of inhibitor leads to rise the enthalpy of the corrosion process. The negative values of entropies of activation ($\Delta S^{\circ}a$) imply that the activated complex in the rate determining step represents an association rather than a dissociation step, meaning that a decrease in disordering takes place on going from reactants to the activated complex [26].

On the other hand, the average difference value of the $E^{\circ}a-\Delta H^{\circ}a$ is 2.7 KJ.mol⁻¹, which is approximately equal to the average value of RT (2.69 KJ.mol⁻¹) at the average temperature (323 K) of the domain studied. This result agrees that the corrosion process is a unimolecular reaction as described by the known Eq. (9) of perfect gas:

$$E^{\circ}a - \Delta H^{\circ}a = RT \quad (9)$$

3.6. Adsorption isotherm and Thermodynamic parameters

It is know that the adsorption process of inhibitor depends on its electronic characteristics, the nature of metal surface, temperature, steric effects and the varying degrees of surface-site activity. In fact, the solvent H₂O molecules could also be adsorbed at the metal/solution interface. In the aqueous solution, the adsorption of inhibitor molecules can be considered as a quasi-substitution process between the inhibitor in the aqueous phase $Inh_{(sol)}$ and water molecules at the electrode surface $H_2O_{(ads)}$ [27]:



where x is the size ratio, that is, the number of water molecules re-placed by one organic inhibitor.

This equation showed that the interaction force between metal and inhibitor must be greater than the interaction force of metal and water molecule. The corrosion adsorption processes can be understood using adsorption isotherm. Langmuir adsorption isotherm is attributing to physisorption or chemisorption phenomenon while Temkin adsorption isotherm gives an explanation about the heterogeneity formed on the metal surface. Chemisorption was attributed to Temkin isotherm [28]. Here, Langmuir, Frumkin and Temkin adsorption isotherms were applied in order to explain the adsorption process of AL oil on the mild steel surface:

$$\text{Langmuir} : \frac{C_{inh}}{\theta} = \frac{1}{K} + C_{inh} \quad (11)$$

$$\text{Temkin} : \text{Ln} \left(\frac{C_{inh}}{\theta} \right) = \text{Ln}K - g\theta \quad (12)$$

$$\text{Frumkin} : \text{Ln} \left(C_{inh} * \left(\frac{\theta}{1-\theta} \right) \right) = \text{Ln}K + g\theta \quad (13)$$

where θ is the surface coverage, K is the adsorption–desorption equilibrium constant, C_{inh} is the concentration of inhibitor and g is the adsorbate parameter.

The dependence of the fraction of the surface covered θ obtained by the ratio $E_w/100$ as function of the AL oil concentration (C_{inh}) was graphically fitted for these various adsorption isotherms.

The linear regression parameters between C/θ and C were listed in Table 6, and the straight lines of C/θ versus C in 1 M HCl at different temperatures are shown in Figure 8. It is evident that all linear correlation coefficients (R^2) are almost equal to 1, and the slope values are also close to 1, which indicates that the adsorption of AL oil on steel surface obeys Langmuir adsorption isotherm. This result showed that the adsorbed molecules occupy only one site and there are no interactions with other adsorbed species [29].

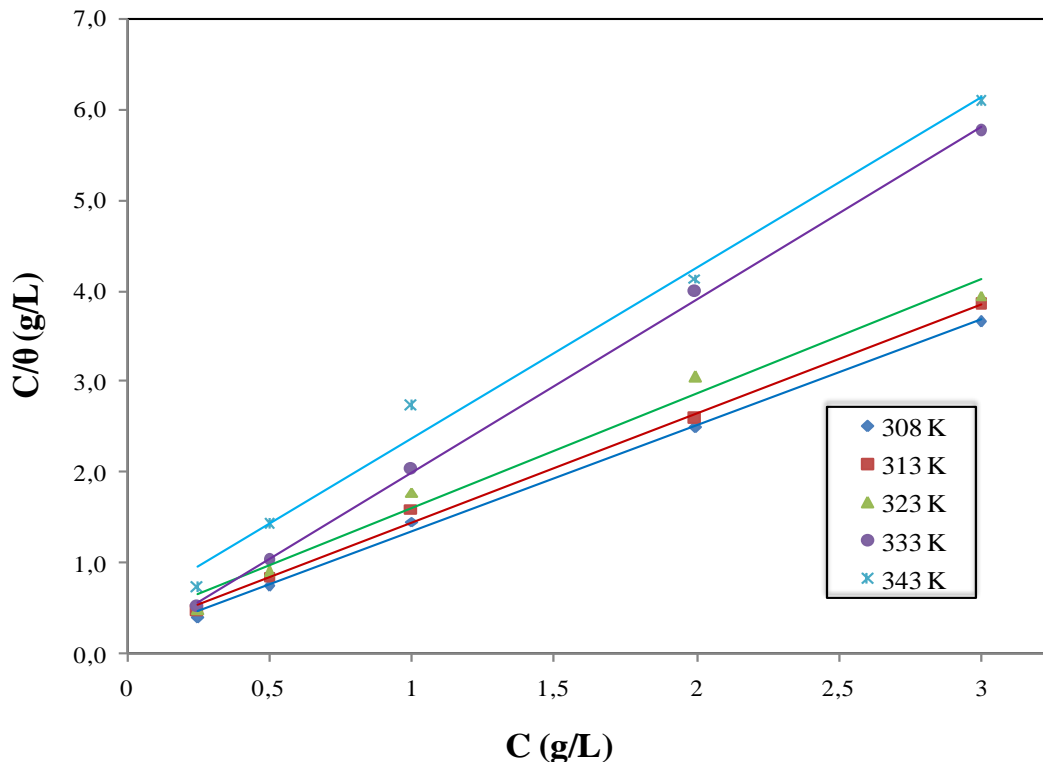


Figure 8: Langmuir adsorption isotherm of *A. leucotrichus* fruit essential oil on the mild steel surface in 1 M HCl at different temperatures.

As shown in Table 6, the adsorptive equilibrium constant (K) decreases with the temperature in 1 M HCl solution, which could be ascribed easily for inhibitor to adsorb on the steel surface at relatively lower temperature. However, when the temperature is gone up, the adsorbed inhibitor tends to desorb from the steel surface. Generally, large value of K is bound up with better inhibition efficiency of a given inhibitor. This is in good agreement with the values of E_w obtained from Figure 2.

Thermodynamic parameters are important to further understand the adsorption process of inhibitor on steel/solution interface. The equilibrium adsorption constant, K is related to the standard Gibb’s free energy of adsorption (ΔG°_{ads}) with the following equation:

$$K = \frac{1}{55.5} \cdot \exp\left(-\frac{\Delta G^\circ_{ads}}{RT}\right) \quad (14)$$

The standard adsorption enthalpy (ΔH°_{ads}) could be calculated based on Van’t Hoff equation [30]:

$$\text{Ln}K = -\frac{\Delta H^\circ_{ads}}{RT} + D \quad (15)$$

where R is the universal gas constant, T is the thermodynamic temperature, D is integration constant, and the value of 55.5 is the concentration of water in the solution in mol/L (10^3 g/L).

The standard adsorption enthalpy ($\Delta H^\circ_{\text{ads}}$) can also be calculated from the Gibbs-Helmholtz equation:

$$\frac{\Delta G^\circ_{\text{ads}}}{T} = \frac{\Delta H^\circ_{\text{ads}}}{T} + k \quad (16)$$

To calculate the enthalpy of adsorption ($\Delta H^\circ_{\text{ads}}$), $\text{Ln}K$ was plotted against $1/T$ (Figure 9) and straight line was obtained with slope equal to $(-\Delta H^\circ_{\text{ads}}/T)$. The variation of $\Delta G^\circ_{\text{ads}}/T$ vs $1/T$ gives straight line with slope equal to $\Delta H^\circ_{\text{ads}}$ (Figure 10).

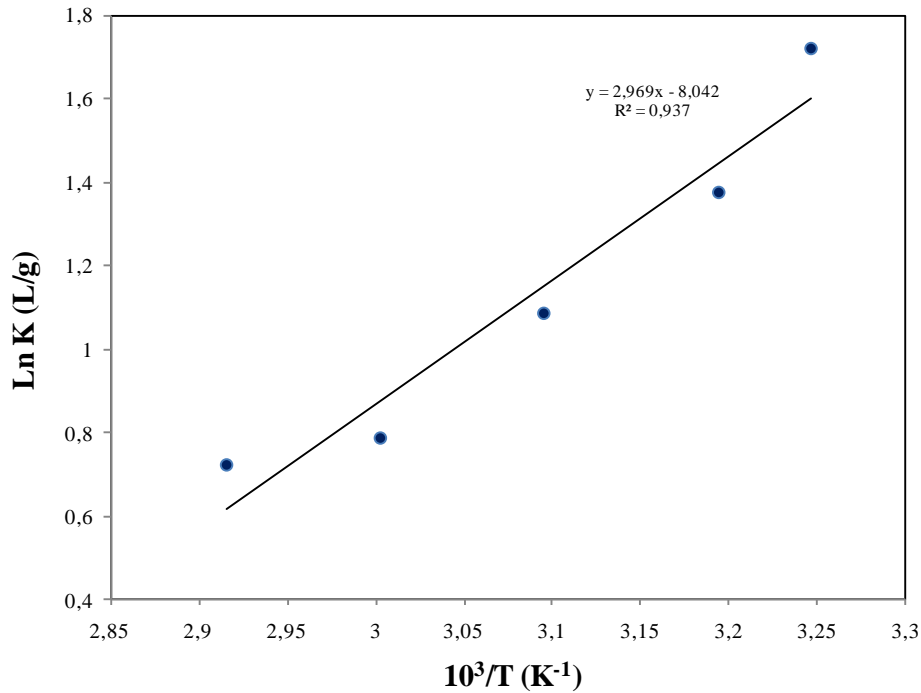


Figure 9: Van't Hoff's plot of $\text{Ln} K$ against $1/T$ for the adsorption of *A. leucotrichus* fruit essential oil onto mild steel.

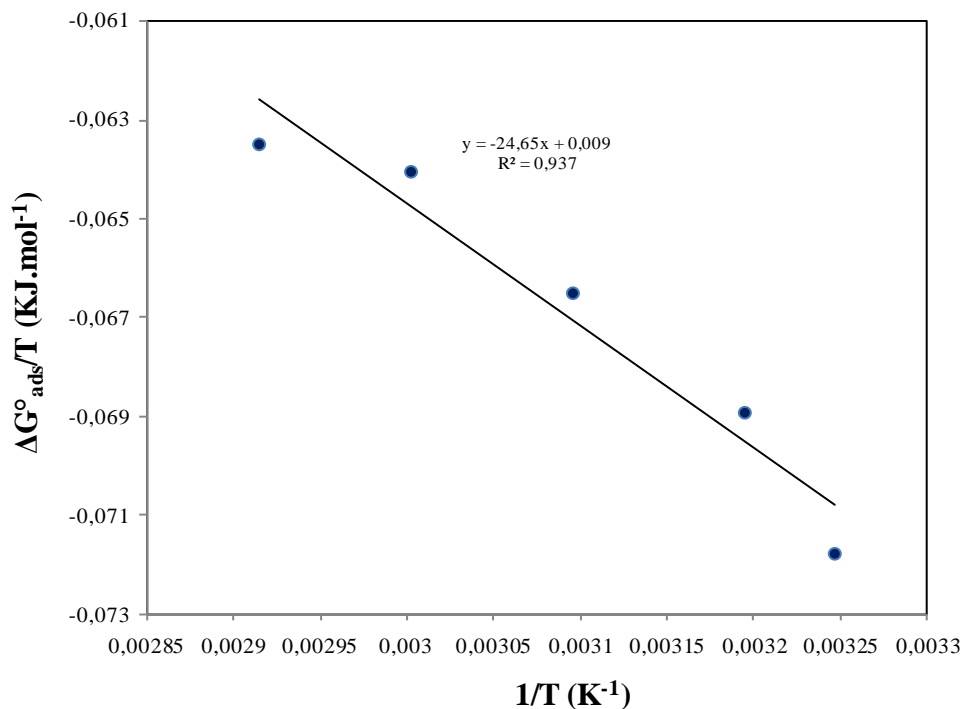


Figure 10: The relationship between $(\Delta G^\circ_{\text{ads}}/T)$ and $1/T$.

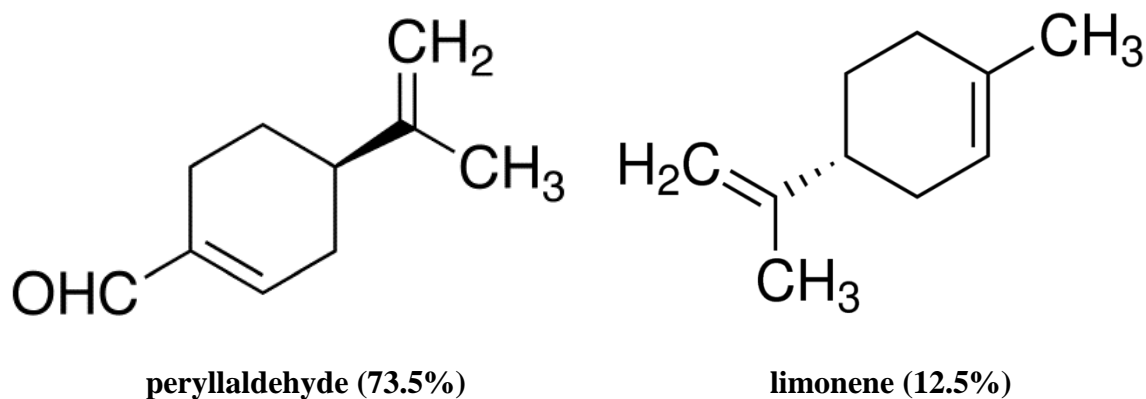
With the obtained both parameters of $\Delta G^{\circ}_{\text{ads}}$ and $\Delta H^{\circ}_{\text{ads}}$, the standard adsorption entropy ($\Delta S^{\circ}_{\text{ads}}$) can be calculated using the following thermodynamic basic Equ. (17):

$$\Delta S^{\circ}_{\text{ads}} = \frac{\Delta H^{\circ}_{\text{ads}} - \Delta G^{\circ}_{\text{ads}}}{T} \quad (17)$$

We limit our study to the qualitative study of adsorption part, we believe that $\Delta G^{\circ}_{\text{ads}}$, $\Delta H^{\circ}_{\text{ads}}$ and $\Delta S^{\circ}_{\text{ads}}$ cannot be computed in the case of oil or extract of natural plants contrary to the use of known molecule.

3.7. Explanation for inhibition.

The *A. leucotrichus* fruit essential oil was dominated by peryllaldehyde (73.5%) and limonene (12.5%). These compounds represent 86% of the total oil and contain oxygen atoms in functional groups (C=O) and π -electrons of the double bonds (C=C), which meets the general characteristics of typical corrosion inhibitors. Accordingly, the inhibitive action of AL oil could be attributed to the adsorption of these compounds on the mild steel surface [35]. The limonene exhibited a good inhibitory effect on steel in HCl solution [36] and aldehyde compounds were widely used [36-38]. However, it is also possible that the minor components might be involved in some type of synergism effect with these two compounds.



Generally, in aqueous acidic solution, the organic molecules of AL essential oil exist either as neutral molecules or in the form of protonated organic molecules (cations). Therefore, two modes of adsorption are considered on the metal surface in acid media. In the first mode, the neutral molecules may be adsorbed on the surface of mild steel through the chemisorption mechanism, involving the displacement of water molecules from the mild steel surface and the sharing electrons between the oxygen atoms and iron. The inhibitor molecules can also adsorb on the mild steel surface because of donor-acceptor interactions between their π -electrons and vacant d-orbitals of surface iron. In second mode, since it is well known that it is difficult for the protonated molecules to approach the positively charged mild steel surface (H_3O^+ /metal interface) due to the electrostatic repulsion. Since Cl^- have a smaller degree of hydration, they could bring excess negative charges near the interface and favour more adsorption of the positively charged inhibitor molecules, the protonated inhibitors adsorb through electrostatic interactions between the positively charged molecules and the negatively charged metal surface. Thus, there is a synergism between adsorbed Cl^- ions and protonated inhibitors [39-42].

Conclusion

A. leucotrichus fruit essential oil acts as good inhibitor for the corrosion of mild steel in 1 M HCl solution. The inhibition action of this essential oil can be attributed to the adsorption of major monoterpene compounds as peryllaldehyde and limonene. From loss measurements, it is clear that inhibition efficiency values increased with increase in inhibitor concentration but decreased with increase in temperature. The results of potentiodynamic measurements revealed clearly that AL oil is a mixed inhibitor for mild steel corrosion in acidic solution. The results of EIS measurements indicated that the charge transfer process mainly controls the corrosion of steel. The value of apparent activation energy increased with the increase in the inhibitor concentration. Enthalpy of

activation reflects the endothermic nature of the mild steel dissolution process. Entropy of activation increased with increasing inhibitor concentration; hence increase in the disorderliness of the system. The adsorption behavior can be described by the Langmuir adsorption isotherm. Gibbs free energy of adsorption, enthalpy of adsorption and entropy of adsorption indicated that the adsorption process is spontaneous and exothermic and the molecules adsorbed on the metal surface by the process of physical adsorption.

Knowledge: This work was done within the framework of the FP7 IRSES project Oil & Sugar project (contract No. 295202) which supported mobility of young researchers between the partners participating to it.

References

1. Liu Q., Zhu. Z.Y., Ke W., Han C.I., Zeng C.L., *Corros Nace.* 57 (2001) 730.
2. FEghbali F., Moayed M.H., Davoodi A., Ebrahimi N., *Corros Sci.* 53(2011) 513.
3. Poongothai N., Ramachandaren T., Natesan M., Murugavel S. C., *Mater. Perfor, NACE Int,* 48(9) (2009) 52.
4. Bouyanzer A., Hammouti B., Majidi L., *Mater. Letters* 60 (2006) 2840.
5. Bouyanzer A., Majidi L., Hammouti B., *Bull. Elect.* 22 (2006) 321.
6. Znini M., Paolini J., Majidi L., Desjobert J.-M., Costa J., Lahhit N., Bouyanzer A., *Res. Chem. Intermed.* 38 (2012) 669.
7. Ouachikh O., Bouyanzer A. , Bouklah M., Desjobert J.-M., Costa J. , Hammouti B., Majidi L., *Surf. Rev. Lett.* 16 (2009) 49.
8. Lahhit N., Bouyanzer A., Desjobert J.-M., Hammouti B., Salghi R., Costa J., Jama C., Bentiss F., Majidi L., *Port. Electroch. Acta.* 29 (2011) 127.
9. Cristofari G., Znini M., Majidi L., Costa J., Hammouti B., Paolini J., *Int. J. Electrochem. Sci.* 7 (2012) 9024.
10. Darriet F., Znini M., Majidi L., Muselli A., Hammouti B., Bouyanzer A., Costa J., *Int. J. Electrochem. Sci.* 8 (2013) 4328.
11. P. Ozenda, *Flore et Végétation du Sahara.* 3^{ème} Ed. CNRS, Paris, (1991) 360.
12. Maberly P. L., *The Plant Book,* Cambridge University Press, Cambridge, (1998).
13. Bellakhdar J., *La pharmacopée marocaine traditionnelle. Médecine arabe ancienne et savoirs populaires.* IBIS Press. (1997) 764.
14. Conseil de l'Europe, *Pharmacopée Européenne,* Maisonneuve S. A. : Sainte Ruffine, (1996).
15. D. Joulain, König, W.A. *The atlas of spectral data of sesquiterpene hydrocarbons.* EbVerlag, Hamburg. (1998).
16. Hochmuth D., Joulain D., König W.A, *Terpenoids and related constituents of essential oils,* Library of Massfinder 2.1, University of Hamburg Institute of organic chemistry Hamburg Germany. (2001).
17. R.P. Adams, *Identification of Essential Oil Components by Gaz Chromatography/Quadrupole Mass Spectroscopy;* Allured Publishing: Carol Stream, (2004).
18. Tsuru T., Haruyama S., Gijutsu B., *Jpn. Soc. Corros. Eng.* 27 (1978) 573.
19. A. Velasco-Negueruela, M.J. Perez-Alonso, P.L. Perez de Paz, J. Pal Paul, J. Sanz. *J. Chromatograph. A,* 1108 (2006) 273.
20. Milton Helio L., Eloisa A. H., Guilherme J. M., *Flav. Fragr, J.* 20 (2005) 462.
21. Satapathy A. K., Gunasekaran G., Sahoo S. C., Amit K., Rodrigues P. V., *Corros. Sci.* 51 (2009) 2848.
22. Fouda A., El-Bendary A., Diabb M., Bakra A., *Mor. J. Chem.* 2 (2014) 302-319.
23. Saranya J., Sounthari P., Kiruthuka A., Parameswari K., Chitra S., *J. Mater. Environ. Sci.* 6 (2015) 425-444
24. Messaadia L., ID El mouden O., Anejjar A., Messali M.; Salghi R., Benali O., Cherkaoui O., Lallam A., *J. Mater. Environ. Sci.* 6 (2015) 598-606.
25. Orubite K. O., Oforka N. C., *Mater. Lett.* 58 (2004) 1772.

26. Samkarapapaavinasam S., Ahmed M. F., *J. Appl. Electrochem.* 22 (1992) 390.
27. Znini M., Cristofari G., Majidi L., Ansari A., Bouyanzer A., Paolini J., Costa J., Hammouti B., *Inter. J. Electrochem. Sci.* 7 (2012) 3959–3981.
28. Wahyuningrum D., Achmad S., Syah Y. M., Buchari B., Bundjali B., Ariwahjoedi A., *Int. J. Electrochem. Sci.* 3 (2008) 164.
29. Cheng S., Chen S., Liu T., Chang X., Yin Y., *Mater. Lett.* 61 (2007) 3279.
30. Libin T., Guannan M., Guangheng L., *Corros. Sci.* 45 (2003) 2251.
31. Khadraoui A., Khelifa A., Boutoumi H., Hammouti B., *Natural Product Research* 28 (2014) 1206-1209
32. Khadraoui A., Khelifa A., Boutoumi H., Hamitouche H., Mehdaoui R., Hammouti B., Al-Deyab S.S., *Int. J. Electrochem. Sci.* 9 (2014) 3334 - 3348.
33. Ali A.I., *J. Mater. Environ. Sci.* 5 (2014) 793-802.
34. El Ouariachi E., Paolini J., Bouklah M., Elidrissi A., Bouyanzer A., Hammouti B., Desjobert J.-M., Costa J., *Acta Metallurgica Sinica (English Letters)*, 23 (2010) 13-20.
35. Faska Z., Bellioua A., Bouklah M., Majidi L., R. Fihri R., Bouyanzer A., Hammouti B., *Monatsh. Chem.* 139 (2008) 1417.
36. Chaieb E., Bouyanzer A., Hammouti B., Berrabah M., *Acta Phys. Chim. Sin.* 25 (2009) 1254-1258
37. Verma C.B., Reddy M.J., Quraishi M.A., *Anal. Bioanal. Electrochem.* 6 (2014) 321-340.
38. Avdeev, Y.G., Kuznetsov, Y.I., Buryak, A.K., *Corrosion Science* 69 (2013) 50-60
39. Mu G. N., Zhao T. P., Liu M., Gu T., *Corrosion.* 52 (1996) 853.
40. Ahamad I., S. Khan, Ansari K. R., Quraishi M. A., *J. Chem. Pharm. Res.* 3 (2011) 703.
41. Yadav M., Kumar S., Sharma U., Yadav P.N., *J. Mater. Environ. Sci.* 4 (5) (2013) 691-700
42. Fouda A.S., Abdallah Y.M., Nabil D., *International Journal of Innovative Research in Science, Engineering and Technology*, 3 N°5 (2014) 12965-82

(2015); <http://www.jmaterenvirosnci.com/>